Inorg. Chem. **2003**, *42*, 2115–2124

1*H*,1*H*,2*H*,2*H*-Perfluoroalkyl-Functionalization of Ni(II), Pd(II), and Pt(II) Mono- and Diphosphine Complexes: Minimizing the Electronic Consequences for the Metal Center

Elwin de Wolf,[†] Ad J. M. Mens,[‡] Onno L. J. Gijzeman,[‡] Joop H. van Lenthe,[§] Leonardus W. Jenneskens,[||] Berth-Jan Deelman,*[,⊥] and Gerard van Koten[†]

Department of Metal-Mediated Synthesis, Debye Institute, Utrecht University, Padualaan 8, 3584 CH Utrecht, The Netherlands, Department of Inorganic Chemistry, Debye Institute, Utrecht University, Sorbonnelaan 16, 3584 CA Utrecht, The Netherlands, Department of Theoretical Chemistry, Debye Institute, Utrecht University, Padualaan 8, 3584 CH Utrecht, The Netherlands, Department of Physical Organic Chemistry, Debye Institute, Utrecht University, Padualaan 8, 3584 CH Utrecht, The Netherlands, and ATOFINA Vlissingen B.V., P.O. Box 70, 4380 AB Vlissingen, The Netherlands

Received June 5, 2002

A series of fluorous derivatives of group 10 complexes MCl_2(dppe) and $[M(dppe)_2](BF_4)_2$ (M = Ni, Pd or Pt; dppe = 1,2-bis(diphenylphosphino)ethane) and *cis*-$PtCl_2(PPh_3)_2$ was synthesized. The influence of *para*-(1*H*,1*H*,2*H*,2*H*-perfluoroalkyl)dimethylsilyl-functionalization of the phosphine phenyl groups of these complexes, as studied by NMR spectroscopy, cyclovoltammetry (CV), XPS analyses, as well as DFT calculations, points to a weak steric and no significant inductive electronic effect. The steric effect is most pronounced for M = Ni and leads in the case of $NiCl_2$(**1c**) (**3c**) and $[Ni(\mathbf{1c})_2](BF_4)_2$ (**7c**) (**1c** = $[CH_2P\{C_6H_4(SiMe_2CH_2CH_2C_6F_{13})\text{-}4\}_2]_2$) to a tetrahedral distortion from the expected square planar geometry. The solubility behavior of $NiCl_2[CH_2P\{C_6H_4(SiMe_{3-b}(CH_2CH_2C_xF_{2x+1})_b)\text{-}4\}_2]_2$ (**3**: b = 1–3; x = 6, 8) in THF, toluene, and *c*-$C_6F_{11}CF_3$ was found to follow the same trends as those observed for the free fluorous ligands **1**. A similar correlation between the partition coefficient (P) of complexes **3** and free **1** was observed in fluorous biphasic solvent systems, with a maximum value obtained for **3f** (b = 3, x = 6, P = 23 in favor of the fluorous phase).

Introduction

Preferential solubility of a transition metal complex in perfluorocarbon solvents is of interest because it allows its separation from nonfluorous components, a feature especially interesting for the recycling of homogeneous catalysts.[1,2] To achieve preferential fluorous phase solubility, one or more perfluoroalkyl groups are usually attached to the ligand system, according to the *like-dissolves-like* principle. Since perfluoroalkyl groups are bulky[3] and highly electron withdrawing,[4] perfluorotail-functionalization of the ligand system is often not trivial, because it can influence the properties of the ligand, which can result in altered reactivity and selectivity. Therefore, several insulating groups have been used to minimize the direct inductive electronic effect that a perfluoroalkyl tail can exert on the metal center.[5] However, small electron-withdrawing effects were still observed for most spacers, e.g., as reflected in a change of ν_{CO} in the IR spectrum of *trans*-$[MCl(CO)(L)_2]$ (M = Rh, Ir; L =

* To whom correspondence should be addressed. E-mail: berth-jan.deelman@atofina.com.
[†] Department of Metal-Mediated Synthesis, Debye Institute.
[‡] Department of Inorganic Chemistry, Debye Institute.
[§] Department of Theoretical Chemistry, Debye Institute.
[||] Department of Physical Organic Chemistry, Debye Institute.
[⊥] ATOFINA Vlissingen B.V.

(1) Cornils, B.; Herrmann, W. A. In *Applied Homogeneous Catalysis with Organometallic Compounds*; Cornils, B., Herrmann, W. A., Eds.; VCH Verlagsgesellschaft mbH, Weinheim, 1996; Chapter 3.1, p 575.
(2) (a) de Wolf, E.; van Koten, G.; Deelman, B.-J. *Chem. Soc. Rev.* **1999**, *28*, 37. (b) Hope, E. G.; Stuart, A. M. *J. Fluorine Chem.* **1999**, *100*, 75. (c) Horváth, I. T. *Acc. Chem. Res.* **1998**, *31*, 641. (d) Curran, D. P. *Angew. Chem., Int. Ed.* **1998**, *37*, 1174. (e) Cornils, B. *Angew. Chem.*, Int. Ed. Engl. **1997**, *36*, 2057.
(3) Kloubek, J. *Colloids Surf.* **1991**, *55*, 191.
(4) Huheey, J. E. *J. Phys. Chem.* **1965**, *69*, 3284.
(5) (a) Horváth, I. T.; Rábai, J. *Science* **1994**, *266*, 72. (b) Smith, D. C.; Stevens, E. D.; Nolan, S. P. *Inorg. Chem.* **1999**, *38*, 5277. (c) Bhattacharyya, P.; Croxtall, B.; Fawcett, J.; Fawcett, J.; Gudmunsen, D.; Hope, E. G.; Kemmitt, R. D. W.; Paige, D. R.; Russell, D. R.; Stuart, A. M.; Wood, D. R. W. *J. Fluorine Chem.* **2000**, *101*, 247.

10.1021/ic025770l CCC: $25.00
Published on Web 02/22/2003

monodentate (fluorous) phosphine).[6] Only a few studies were reported in which the influence of a perfluoroalkyl group on the metal center of transition metal complexes was investigated in more detail, using electrochemical techniques,[7] density functional theory (DFT) calculations[8] and X-ray photoelectron spectroscopy (XPS).[9]

We recently reported on several fluorous derivatives of 1,2-bis(diphenylphosphino)ethane (dppe) (**1a** and **1c**−**f**)[10] and fluorous monophosphines such as **2b**[11] containing a $-SiMe_{3-b}(CH_2CH_2-)_b$-spacer. The metal (predominantly Rh(I)) complexes containing these fluorous ligands were used as homogeneous catalysts for the hydrogenation of 1-alkenes and 4-octyne.[12] Interestingly, these catalysts displayed similar activity compared to their nonfluorous counterparts.

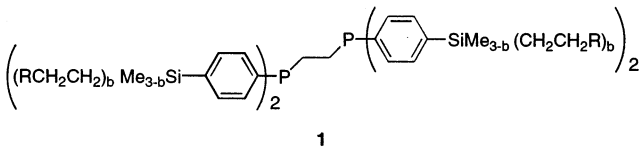

1

1a: $b = 0$
1b: R = C_6H_{13}, $b = 1$
1c: R = C_6F_{13}, $b = 1$
1d: R = C_8F_{17}, $b = 1$
1e: R = C_6F_{13}, $b = 2$
1f: R = C_6F_{13}, $b = 3$

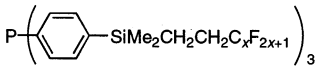

2

2a: $x = 1$
2b: $x = 6$

In this paper, a quantitative investigation of the effects of *para*-(1*H*,1*H*,2*H*,2*H*-perfluoroalkyl)silyl-functionalization of the phosphine phenyl groups on the steric and electronic properties of d^8-metal(II) complexes is presented using the new transition metal complexes MCl_2(**1**) and $[M(\mathbf{1})_2](BF_4)_2$ (M = Ni, Pd or Pt) and *cis*-$PtCl_2$(**2**) (Scheme 1).[12b] Apart from the previously reported *para*-$SiMe_3$ derivative **1a**, which was used as a reference compound, two new ligands containing a *para*-$SiMe_2CH_2CH_2CF_3$ (**2a**) and a *para*-$SiMe_2C_8H_{17}$ (**1b**) substituent, respectively, were prepared which allow the separate study of electronic (**2a**) and steric properties (**1b**) of a *para*-$SiMe_2R$ substituent. Also, the solubility behavior and partitioning of the various fluorous nickel complexes $NiCl_2$(**1**) in a fluorous biphasic solvent system are presented.

Scheme 1

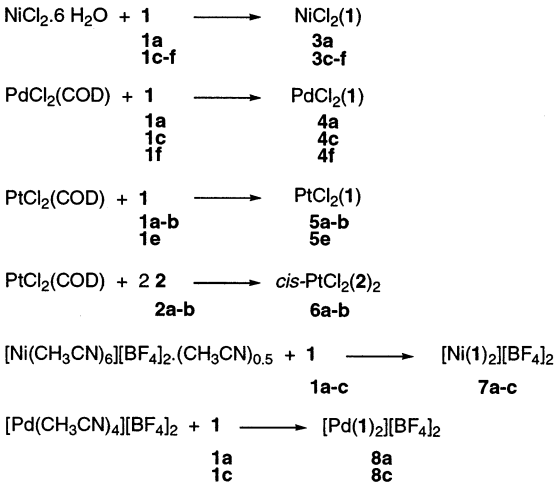

Results

Synthesis. The neutral fluorous complexes MCl_2(**1**) (M = Ni (**3**), Pd (**4**), Pt (**5**)), *cis*-$PtCl_2$(**2**) (**6**), and the dicationic complexes $[M(\mathbf{1})_2](BF_4)_2$ (M = Ni (**7**), Pd (**8**)) were synthesized analogously to published procedures[13,14] with some modifications (see Experimental Section) (Scheme 1). In the case of **3d** and **3f**, the diphosphines (**1d** and **1f**) were added as solution in $CF_3C_6H_5$ (BTF). For the preparation of highly fluorous **3f**, also a BTF/MeOH solvent mixture had to be used to dissolve the starting compound $[Ni(H_2O)_6]Cl_2$ as well as to prevent immediate precipitation of the reactants and (side)-products. Similarly, **4f** was prepared in a fluorous biphasic system consisting of CH_2Cl_2 and *c*-$C_6F_{11}CF_3$ (PFMCH).

All complexes were characterized by ^1H and ^{31}P NMR spectroscopy as well as elemental analyses. In addition, **3c**−**d**, **4c**, **5c**, **7c**, and **8c** were characterized by ^{19}F NMR spectroscopy. The ^1H NMR spectra of complexes containing the highly fluorous ligand **1e** or **1f** displayed broad peaks (multiplicities were not resolved).[15] All ^{31}P and ^{195}Pt NMR chemical shifts and $^1J_{PtP}$ coupling constants of the fluorous compounds are close to the values measured for complexes containing the corresponding nonsubstituted as well as trimethylsilyl-substituted ligands (Table 1 and Experimental Section) indicating similar (*cis*-)square planar structures for

(6) (a) Alvey, L. J.; Meier, R.; Soós, T.; Bernatis, P.; Gladysz, J. A. *Eur. J. Inorg. Chem.* **2000**, 1975. (b) Klose, A.; Gladysz, J. *Tetrahedron: Asymmetry* **1999**, *10*, 2665. (c) Smith, D. C.; Stevens, E. D.; Nolan, S. P. *Inorg. Chem.* **1999**, *38*, 5277. Bhattachrayya, P.; Corxtall, B.; Fawcett, J.; Facett, J.; Gudmunsen, D.; Hope, E. G.; Kemmitt, R. D. W.; Paige, D. R.; Russell, D. R.; Stuart, A. M.; Wood, D. R. W. *J. Fluorine Chem.* **2000**, *101*, 247.
(7) Hughes, R. P.; Trujillo, H. A. *Organometallics* **1996**, *15*, 286.
(8) (a) Banet Osuma, A. M.; Chen, W.; Hope, E. G.; Kemmitt, R. D. W.; Paige, D. R.; Stuart, A. M.; Xiao, J.; Xu, L. *J. Chem. Soc., Dalton Trans.* **2000**, 4052. (b) Szlávik, Z.; Tárkaýi, G.; Gömöry, A.; Tarczay, G.; Rábai, J. *J. Fluorine Chem.* **2001**, *108*, 7.
(9) (a) Goll, J. G.; Moore, K. T.; Ghosh, A.; Therien, M. J. *J. Am. Chem. Soc.* **1996**, *118*, 8344. (b) Moore, K. T.; Fletcher, J. T.; Therien, M. J. *J. Am. Chem. Soc.* **1999**, *121*, 5196.
(10) de Wolf, E.; Richter, B.; Deelman, B.-J.; van Koten, G. *J. Org. Chem.* **2000**, *65*, 5424.
(11) Richter, B.; de Wolf, E.; van Koten, G.; Deelman, B.-J. *J. Org. Chem.* **2000**, *65*, 3885.
(12) (a) de Wolf, E.; Spek, A. L.; Kuipers, B. W. M.; Philipse, A. P.; Meeldijk, J. D.; Bomans, P. H. H.; Frederik, P. M.; Deelman, B.-J.; van Koten, G. *Tetrahedron* **2002**, 58, 3911. (b) Richter, B.; de Wolf, A. C. A.; van Koten, G.; Deelman, B.-J. (ATOFINA) PCT Int. Appl. WO 0018444, 2000. (c) Richter, B.; Spek, A. L.; van Koten, G.; Deelman, B.-J. *J. Am. Chem. Soc.* **2000**, *122*, 3945. (d) van den Broeke, L. J. P.; Goetheer, E. L. V.; Verkerk, A. W.; de Wolf, E.; Deelman, B.-J.; van Koten, G.; Keurentjes, J. T. F. *Angew. Chem., Int. Ed.* **2001**, *40*, 4473.
(13) (a) Booth, G.; Chatt, J. *J. Chem. Soc.* **1965**, 3238. (b) Broadwood-Strong, G. T. L.; Chaloner, P. A.; Hitchcock, P. B. *Polyhedron* **1993**, *12*, 721. (c) Drew, D.; Doyle, J. R.; Shaver, A. G. *Inorg. Synth.* **1972**, *13*, 47.
(14) Miedaner, A.; Curtis Haltiwanger, R.; DuBois, D. L. *Inorg. Chem.* **1991**, *30*, 417.
(15) No significant changes in line broadening were observed upon heating to 50 °C.

Table 1. ^{31}P NMR Data of $PtCl_2$(**1**) and *cis*-$PtCl_2$(**2**) and Their Nonsubstituted Analogues

compd	δ (^{31}P) (ppm)[a]	$^1J_{PtP}$ (Hz)	δ (^{195}Pt) (ppm)[a]
$PtCl_2$(dppe)[b]	40.9	3618	−4572
5a[c]	41.8	3612	−4573
5c	41.9	3604	−4570
5e	42.0[d]	3593	*e*
cis-$PtCl_2(PPh_3)_2$	15.2	3666	−4431
6a	14.1	3665	−4418
6b	14.1	3663	−4420

[a] In $CDCl_3$ unless noted otherwise. [b] ^{31}P NMR data in $(CD_3)_2CO$: δ 42.8 ($^1J_{PtP}$ = 3594 Hz). [c] ^{31}P NMR data in $(CD_3)_2CO$: δ 47.4 ($^1J_{PtP}$ = 3588 Hz). [d] In $CDCl_3/CF_3C_6H_5$ 1:1 (v/v). [e] Not soluble in $CDCl_3$.

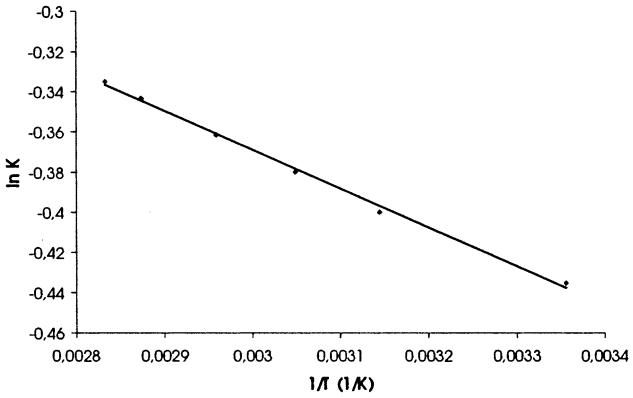

Figure 1. van't Hoff plot of variable temperature ^{31}P NMR measurements on **7c**.

the fluorous compounds and their nonfluorous analogues. The only exceptions were the ionic bis(diphosphine) nickel complexes **7**; whereas a single resonance in the ^{31}P NMR spectra of $[Ni(dppe)_2](BF_4)_2$ and **7a** was observed, two singlet resonances were detected for **7c** at δ = 54.9 and 55.0 ppm (3:1 ratio),[16] probably indicating that at least two different isomers of **7c** are present in solution (vide infra). The 3:1 ratio increased upon increasing the temperature. From the different ratios of these two peaks in ^{31}P NMR obtained upon heating gradually from 25 to 80 °C, the thermodynamic parameters ($\Delta H°$ = 2.2 kJ/mol and $\Delta S°$ = 1.7 J/K mol) were obtained from a van't Hoff plot (Figure 1) which also confirmed that the two isomers of **7c** are indeed in equilibrium. The modest value of $\Delta H°$ also suggests that the two isomers are structurally closely related (vide infra).

Solubility and Partitioning. For immobilization and fluorous phase extraction of fluorous complexes in a fluorous phase, their solubility characteristics and partitioning behavior in a fluorous biphasic system are important properties. To this end, the solubility and partitioning of $NiCl_2$(dppe) and complexes **3** in a biphasic toluene/PFMCH (1:1) solvent mixture were studied (Table 2). It was found that the solubility of $NiCl_2$(dppe) in THF and toluene increased by an order of magnitude upon *para*-trimethylsilyl-functionalization of the dppe ligand (**3a**). Interestingly, when 4 *para*-$SiMe_2CH_2CH_2C_6F_{13}$ groups were attached (i.e., as in **3c**), the solubility of the nickel complex in THF increased even further, whereas the solubility in toluene decreased and no solubility in PFMCH could be detected. This behavior has been observed for the free ligand (**1c**) as well.[10] When the number of perfluoroalkyl tails was further increased from 4 to 8 or 12 per complex (e.g., **3e** or **3f**), both the solubility in THF and toluene decreased, and now, most importantly, the solubility in PFMCH increased dramatically. Similar trends in solubility have been observed previously for the free ligands **1a**,**c**,**e**−**f**.[10]

Not withstanding the described general trends, a large difference in the absolute solubility of free **1d** and **3d** was observed. Whereas **1d** was hardly soluble in THF, toluene, and PFMCH, its nickel complex **3d** displayed high solubility in THF, moderate solubility in toluene, and limited solubility in PFMCH. By considering both the solubility behavior and the weight percentage of fluorine of the various complexes, the fluorous character of **3d** can be placed between that of **3c** and **3e**. This is corroborated by the earlier observation that an increase of the number of perfluoroalkyl tails is more effective for obtaining good solubility in fluorous solvents than an increase of the length of the tail.[10,11,12c] Although not studied quantitatively, similar solubility behavior was observed for the fluorous complexes **4**−**8**, i.e., high solubility in polar organic solvents and insolubility in fluorous solvents for complexes containing **1a**, and low solubility in organic solvents accompanied with high solubility in fluorous solvents for complexes containing **1e** or **1f**.

The most important parameter for recycling of the complexes by fluorous biphasic separation techniques is their partition coefficient *P* in fluorous biphasic solvent combinations ($P = c_{\text{fluorous phase}}/c_{\text{organic phase}}$). The partition coefficients of **3** and those of free **1** parallel the solubility properties (vide supra); i.e. an increase of the weight percentage of fluorine in the ligand or complex results in a higher affinity for the fluorous phase. As observed for the free fluorous ligand, a maximum partition coefficient was observed for complex **3f** with the highest fluorine content (61.8 wt % F; P = 23). Although its fluorophilicity[17] is still modest, it makes **3f** the most interesting candidate as an alternative for $NiCl_2$(dppe) in fluorous biphasic separation strategies. Ligand **1f** was also recently employed in rhodium-catalyzed hydrogenation where recycling efficiencies better than 99.9% have been obtained.[12b]

Electronic and Conformational Study. The ^{31}P NMR chemical shift of platinum phosphine complexes can be unreliable as an indicator for electronic or steric influences exerted by the ligands.[18] The $^1J_{PtP}$ coupling constant, which is also easily obtained, is a more reliable probe for quantifying such influences.[19] In particular, the $^1J_{PtP}$ coupling constant is known to correlate well with the Hammett constant of the *para*-substituent on the aryl ring[20] and in the case of

(16) Despite several attempts to grow single crystals of **7c**, no crystals suitable for X-ray crystal structure determination were obtained, which might possibly be caused by disorder and the presence of more than one structure in the solid state.

(17) Garelli, N.; Vierling, P.; Fischel, J. L.; Milano, G. *Eur. J. Med. Chem.* **1993**, *28*, 235.
(18) Atherton M. J.; Fawcett, J.; Hill, A. P.; Holloway, J. H.; Hope, E. G.; Russell, D. R.; Saunders: G. C.; Stead, R. M. J. *J. Chem. Soc., Dalton Trans.* **1997**, 1137.
(19) (a) Pregosin, P. S. *Coord. Chem. Rev.* **1982**, *44*, 247. (b) Goel, R. G. *Inorg. Nucl. Chem. Lett.* **1979**, *15*, 437.
(20) Cobley, C. J.; Pringle, P. G. *Inorg. Chim. Acta* **1997**, *265*, 107.

Table 2. Solubility and Partition Coefficients of $NiCl_2$(dppe) and $NiCl_2[\{CH_2P(C_6H_4\text{-}SiMe_{3-b}(CH_2CH_2C_xF_{2x+1})_b)_2\}_2]$

			solubility[a]						
			THF		toluene		PFMCH		
compd	*x*	*b*	(g/L)	(mol/L)	(g/L)	(mol/L)	(g/L)	(mol/L)	P^b
$NiCl_2$(dppe)			3	0.008	<0.2	<0.0005	*c*	*c*	*c*
3a		0	130	0.154	96	0.114	*c*	*c*	0.0
3c	6	1	816	0.381	28	0.013	<0.2	<0.00009	1.6
3d	8	1	212	0.083	8	0.003	4	0.002	3.7
3e	6	2	91	0.026	5	0.001	124	0.036	8
3f	6	3	9	0.002	<0.2	<0.00004	>400[d]	>0.083[d]	23

[a] Expressed as the amount of phosphine which can be dissolved in 1 L of pure solvent at 25 °C. Determined by gravimetric methods (PFMCH = perfluorocyclohexane). [b] In a 1:1 (v/v) mixture of PFMCH and toluene at 0 °C ($P = c_{\text{fluorous phase}}/c_{\text{organic phase}}$). Determined by gravimetric methods. The estimated error is ±1 in the last digit. [c] Not determined. [d] Compound **3f** is completely miscible with PFMCH.

diphosphine ligands also with the P−Pt−P bite angle.[21] In addition, the $^1J_{PtP}$ value may be sensitive to the presence of bulky groups, in analogy to observations for the $^1J_{SeP}$ coupling constant.[19,22]

The *para*-trimethylsilyl substituted phosphine derivative of $PtCl_2$(dppe) (**5a**) (Table 1) shows a slightly lower $^1J_{PtP}$ coupling constants compared to its nonsubstituted derivative. A further small decrease in the $^1J_{PtP}$ coupling constant was found for fluorous **5c** and **5e** containing 4 or 8 perfluoroalkyl tails, respectively, although an effect of the different solvent needed to dissolve **5e** cannot be excluded. A similar trend was observed when the $^1J_{PtP}$ coupling constants of nonfluorous *cis*-$PtCl_2(PPh_3)_2$ and fluorous **6a**−**b** were compared which may well correspond to a progressively increasing electron-withdrawing character of the *para*-silyl-substituent. It is clear that the effect is modest, however.

Also, the metal chemical shifts of transition metal complexes are known to be very sensitive probes for changes in the steric and electronic environment.[23] Considering the broad chemical shift window of ^{195}Pt NMR and the high sensitivity for small structural or electronic variations, the nearly identical ^{195}Pt NMR chemical shifts found for both the diphosphine complexes **5a**,**c**,**e** and bis(monophosphine) complexes **6a**−**b** compared to their nonsubstituted analogues further demonstrate that *para*-trimethylsilyl- or *para*-(1*H*,1*H*,2*H*,2*H*-perfluoroalkyl)dimethylsilyl-functionalization does not significantly affect the electronic and/or geometric properties of the platinum metal center.

As a further technique to study the electronic environment of the metal center, the electrochemical behavior of the nickel and palladium complexes **7** and **8** was investigated by cyclic voltammetry (CV) (Table 3). Two reduction waves were observed for all *para*-silyl-substituted nickel complexes **7**, similar to what was reported for $[Ni(dppe)_2](BF_4)_2$, which is again indicative of the closely related electronic properties of the metal centers.[14] However, whereas the first reduction wave of $[Ni(dppe)_2]^{2+}$ to $[Ni(dppe)_2]^{+}$ is quasireversible at high scan rates,[14] an irreversible first reduction was observed for the *para*-silyl-substituted derivatives. The second reduction to the corresponding Ni(0)-species is reversible only for the nonsubstituted and trimethylsilyl-substituted compounds. For **7b**−**c** also the second reduction was irreversible, showing that apparently attachment of a large group rather than specific attachment of a perfluoroalkyl tail affects the reversibility. Possibly, the size of the molecule affects the reversibility of the reduction process, although subsequent reaction of the formed Ni(I)-radical with a functional group (e.g., C−Si, C−F) cannot be excluded. Although CV is often used to monitor electronic effects of substituents, the (ir)reversibility of the reductions studied also depends on the chemical reactivity of the complexes generated. Therefore, the different reversibility of the reductions of the silyl-substituted complexes compared to their nonsubstituted analogues is less important for the study of the electronic and steric influence of a (fluorous) silyl-substituent in the starting complexes.

Table 3. CV Data[a] for *p*-Silyl-Substituted Derivatives of $[M(dppe)_2](BF_4)_2$ (M = Ni, Pd)

compd	$E_{1/2}$ (−1/−2)[b]	E_{onset} (−1/−2)[c]	$E_{1/2}$ (0/−1)[b]	E_{onset} (0/−1)[b]
$[Ni(dppe)_2](BF_4)_2$	−0.73 (80)	−0.56	−0.93 (84)	−0.69
7a	*d*	−0.55	−0.94 (90)	−0.66
7b	*d*	−0.56	-*d*	−0.72
7c	*d*	−0.31	*d*	−0.51
	$E_{1/2}$ (0/−2)	E_{onset} (2/1)[c]	$E_{1/2}$ (1/0)[b]	E_{onset} (1/0)[b]
$[Pd(dppe)_2](BF_4)_2$	−1.04 (35)[e]		*f*	
8a	*d*	−0.58	*d*	−0.99
8c	*d*	−0.81	*d*	−1.07

[a] All peaks (reported in V) are referenced to the ferrocene/ferrocinium couple in $MeCN/CH_2Cl_2$ 1:1. Voltammograms were measured at 50 mV/s. [b] Numbers in brackets indicate the peak to peak separation (ΔE) at 50 mV/s in mV. [c] Similar values were obtained for scan rates of 20 and 100 mV/s. [d] Irreversible reduction. [e] Compound is insoluble in $MeCN/CH_2Cl_2$ 1:1. Data from ref 14 in DMSO, E_{onset} not given. [f] Not observed.

Since the onset values of the reduction waves were found to be independent of experimental conditions (scan rate, potential window, etc.), the onset reduction potentials can be used for comparison of the substituted fluorous and nonfluorous compounds with their nonsubstituted parent complex. All nickel complexes, except **7c**, displayed similar onset values for both the first and the second reduction wave, respectively. The less negative reduction potentials found for **7c** show that the fluorous complex is more easily reduced, which could correspond to a lower electron density on the metal center.

(21) Anderson, G. K.; Davies, J. A.; Schoeck, D. L. *Inorg. Chim. Acta* **1983**, *76*, L251.
(22) Allen, D. W.; Taylor, B. F. *J. Chem. Soc., Dalton Trans.* **1982**, 51.
(23) (a) Loggin, P. L.; Goodfellow, R. J.; Haddock, S. R.; Taylor, B. F.; Marshall, I. R. H. *J. Chem. Soc., Dalton Trans.* **1976**, 459. (b) Pregosin, P. S. *Coord. Chem. Rev.* **1982**, *44*, 247. (c) Hope, E. G.; Levason, W.; Powell, N. A. *Inorg. Chim. Acta* **1986**, *115*, 187.

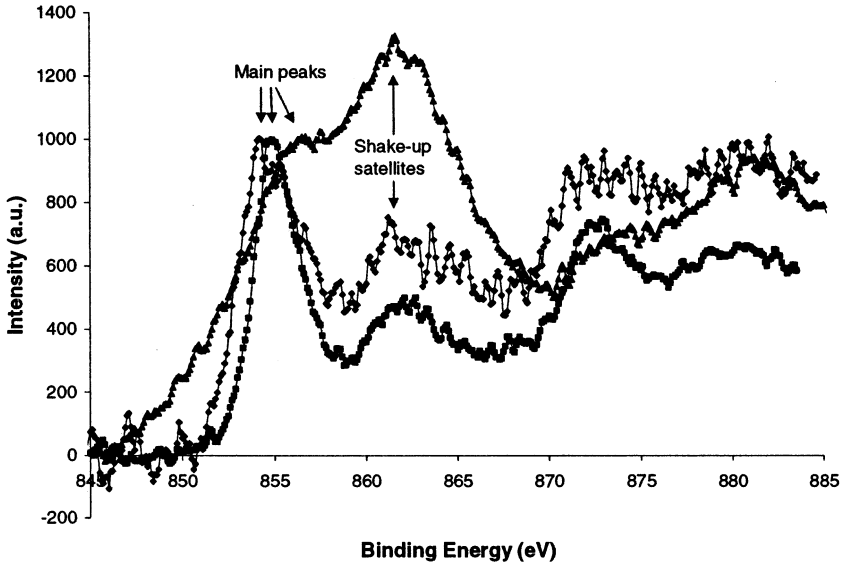

Figure 2. XPS spectra of $NiCl_2$(dppe) (■), **3a** (◆), and **3c** (▼). Spectra were referenced to C_{1s} = 285.0 eV. The intensities of the $2p_{3/2}$ peaks were scaled to 1000 au.

Two reduction processes were observed in the cyclic voltammograms of both **8a** and **8c**, whereas only a single two-electron reversible reduction wave to $[Pd(dppe)_2]^0$ was reported for $[Pd(dppe)_2]^{2+}$.[14] Furthermore, these two reduction waves observed for **8a** and **8c** turned out to be irreversible, in constrast to the reduction behavior of $[Pd(dppe)_2]^{2+}$. The completely different reduction behavior of the *para*-silyl-substituted palladium complexes **8a** and **8c** is most probably caused by different reduction kinetics or a different reactivity of the species resulting from their reduction compared to the species resulting from reduction of their nonsubstituted analogue $[Pd(dppe)_2]^{2+}$ (vide supra).

To further monitor the possible occurrence of an electron-withdrawing effect of the perfluoroalkyl groups on the metal center,[24] XPS measurements were performed on **4**, **5**, and **8** (Table 4) and on **3** and **7** (Table 5).[25,26] Very similar metal as well as phosphorus electron binding energies were found for the complexes containing nonsubstituted dppe, *para*-trimethylsilyl-substituted **1a**, and *para*-(1*H*,1*H*,2*H*,2*H*-perfluorooctyl)dimethylsilyl-substituted **1c**, respectively.

In the XPS spectra of nickel complexes, both the observed electron binding energies and the shape of the signals are important, because of the possible appearance of shake-up satellites.[27] The XPS spectra for nonfluorous $NiCl_2$(dppe) and **3a** are very similar (Table 5 and Figure 2). This observation is also valid for their cationic analogues **7**. However, the shapes of the signals of both fluorous **3c** and **7c** are very different from their respective nonfluorous analogues containing nonsubstituted dppe or trimethylsilyl-substituted **1a**; i.e., relatively high shake-up satellite intensity was observed for the fluorous compounds (Figure 2). Since no or low shake-up satellite intensity is usually observed for square planar nickel complexes,[27,28] the high shake-up satellite intensity observed in the XPS spectra of fluorous **3c** and **7c**

Table 4. XPS Data[a] of $PdCl_2$(**1**) (**4**), $[Pd(\mathbf{1})_2](BF_4)_2$ (**8**), $PtCl_2$(**1**) (**5**), and Their Nonsubstituted Analogues

	binding energy (eV)		
compd	P_{2p}	$Pd_{3d_{5/2}}$	$Pd_{3d_{3/2}}$
$PdCl_2$(dppe)	132.0	338.4	343.6
4a	132.1	338.4	343.6
4c[b]	132.2	338.2	343.4
$[Pd(dppe)_2](BF_4)_2$	131.9	338.7	343.9
8a	132.3	338.7	344.0
8c[b]	132.3	338.7	344.0
	P_{2p}	$Pt_{4f_{7/2}}$	$Pt_{4f_{5/2}}$
$PtCl_2$(dppe)	132.0	73.3	76.5
5a	132.3	73.6	76.8
5c[b]	132.3	73.4	76.3

[a] Peaks referenced to C_{1s} = 285.0 eV. [b] Extra C_{1s} peak observed at 292.0 eV for $(CF_2)_x$.

Table 5. XPS Data[a] of $NiCl_2$(**1**) (**3**), $[Ni(\mathbf{1})_2](BF_4)_2$ (**7**), and Their Nonsubstituted Analogues

	binding energy (eV)				
compd	P_{2p}	$Ni_{2p_{3/2}}$[b]	$SAT_{2p_{3/2}}$	$Ni_{2p_{1/2}}$	$SAT_{2p_{1/2}}$
$NiCl_2$(dppe)	132.0	854.9 (2.7)	862.1	872.5	880.4
3a	132.1	854.5 (3.5)	861.6	872.7	880.5
3c[c]	132.8	855.8 (8.2)[d]	862.3[d]	874.0	881.0
$[Ni(dppe)_2](BF_4)_2$	132.0	855.4 (2.2)	858.4	872.6	878.6
7a	131.8	855.1 (2.9)	*e*	872.3	878.1
7c[c]	132.2	854.6 (6.8)[d]	861.4[d]	873.3	881.0

[a] Peaks referenced to C_{1s} = 285.0 eV. [b] Full width at half-maximum given in parentheses. [c] Extra C_{1s} peak observed at 292.0 eV for $(CF_2)_n$. [d] Values obtained after deconvolution of overlapping $2p_{3/2}$ peak and its satellite into two peaks. [e] Not observed.

(24) (a) Leigh, G. J.; Bremser, W. *J. Chem. Soc., Dalton Trans.* **1972**, 1216. (b) Andreocci, M. V.; Mattogno, G.; Zanoni, R.; Giannoccaro, P.; Vasapollo, G. *Inorg. Chim. Acta* **1982**, *63*, 225. (c) Peuckert, M.; Keim, W.; Storp, S.; Weber, R. S. *J. Mol. Catal.* **1983**, *20*, 115. (d) Gassman, P. G.; Winter, C. H. *J. Am. Chem. Soc.* **1986**, *108*, 4228. (e) Gassman, P. G.; Deck, P. A.; Winter, C. H.; Dobbs, D. A.; Cao, D. H. *Organometallics* **1992**, *11*, 959.

(25) Nefedov, V. I.; Porai-Koshits, M. A. *Mater. Res. Bull.* **1972**, *7*, 1543.

(26) Since **7b** is an oil, no XPS data from this compound can be obtained.

(27) A shake-up electron with an apparent higher binding energy is observed when apart from normal ionization from a 2p orbital, another electron is excited to a higher lying orbital. For nickel, this extra excitation is ascribed to a 3d−4s transition. Since this transition is forbidden for diamagnetic square planar d^8 complexes, usually low shake-up satellite intensity is observed for such complexes. See: Matienzo, L. J.; Yin, L. I.; Grim, S. O.; Swartz, W. E. *Inorg. Chem.* **1973**, *12*, 2762.

Table 6. Mulliken Populations of $[NiCl_2\{(4\text{-R-}C_6H_4)_2PCH_2CH_2P(C_6H_4\text{-}4\text{-R})_2\}]$ Calculated by DFT[a]

R	Hammett param (σ_p)	Mulliken populations	
		Si	Cl
CF_3	0.53		−0.41
F	0.06		−0.42
H	0.00		−0.43
SiH_3	0.00[b]	0.62	−0.43
$SiMe_2CH_2CH_2CF_3$		1.43	−0.43
$SiMe_2CH_2CH_2C_6F_{13}$ (**3c**)		1.43	−0.43
OMe	−0.27		−0.44
NH_2	−0.66		−0.45

[a] Mulliken populations of Ni (0.75) and P (0.55) similar for all compounds. [b] Hammett parameter of $-SiMe_3$.

is most likely caused by tetrahedral distortion of these complexes. Furthermore, deconvolution of the overlapping $2p_{3/2}$ peak and its shake-up satellite shows that also the full width at half-maximum (fwhm) ($\Delta E_{1/2}$) is much larger for fluorous compounds **3c** and **7c**. This indicates that both of the fluorous nickel compounds adopt at least two geometries in the solid state.[16] Further deconvolution for **7c** of the main peak into two peaks, in line with the ^{31}P NMR spectrum of **7c**, gave peaks at 851.9 and 855.3 eV (fwhm = 5.8 and 5.0 eV, respectively) in a 1:2 ratio.

Finally, a possible inductive electronic influence of *para*-(1*H*,1*H*,2*H*,2*H*-perfluoroalkyl)dimethylsilyl-functionalization was studied using density functional theory (DFT) calculations on *para*-substituted derivatives of $NiCl_2$(dppe) and determination of the atomic population distributions (Table 6). Similar slightly distorted, square planar structures ($\angle$*trans*-Cl−Ni−P = 175 °) were found for all compounds.

Interestingly, electron-withdrawing (CF_3, F) or electron-donating (OMe, NH_2) substituents influence the Mulliken populations on the anionic chloride ligands rather than the populations of the nickel (0.75) and phosphorus atoms (0.55), which hardly varied over the range of compounds studied. Except for a *para*-F-substituent, a linear relationship between the Hammett parameter (σ_p) and the Mulliken population on the chlorine atoms was found. It seems that changes of the population on the phosphorus and nickel atoms are compensated for by variation of the electron populations on the chloride ligands. Most importantly, the Mulliken populations on the P, Ni, and Cl atoms of the $-SiH_3$-, $-SiMe_2CH_2CH_2CF_3$-, and $-SiMe_2CH_2CH_2C_6F_{13}$-substituted nickel complexes are essentially identical. It was previously shown by DFT calculations[8] and by IR spectroscopy on a series of *trans*-$[MCl(CO)(L)_2]$ complexes[6] (M = Rh, Ir; L = monodentate (fluorous) phosphine) that *para*-C_xF_{2x+1}- and *para*-$(CH_2)_nC_xF_{2x+1}$-substituents (n = 2, 3) directly attached to the aryl ring exert a (small) electron-withdrawing effect on the phosphorus donor atom. The results of the calculations presented here are further support for the idea that the electron-withdrawing effect of the perfluoroalkyl tail is compensated for by the silicon atom of the $-SiMe_2CH_2CH_2$- spacer. The electron-withdrawing effect of the perfluoroalkyl tail only becomes apparent when comparing the Si Mulliken populations of the $-SiH_3$ and $-SiMe_2CH_2CH_2C_xF_{2x+1}$ (x = 1, 6) moieties.

To further study the relative energies of possible geometric distortions that were observed by XPS for **3c** and **7c**, constrained, tetrahedrally distorted structures of $[Ni(dppe)_2]^{2+}$ were calculated by DFT. The energies of the highest occupied molecular orbital (HOMO) and lowest unoccupied molecular orbital (LUMO) and the relative, calculated total energies are shown in Figure 3a,b. The energy of the HOMO gradually increases upon tetrahedral distortion, whereas the energy of the LUMO only decreases after a maximum at slightly distorted structures ($\angle$*trans*-P−Ni−P = 176 °). For this conformation, the total energy shows a minimum, in agreement with extended Hückel calculations on $[Ni(PH_3)_4]^{2+}$.[14] Subsequently, the total energy gradually increases upon tetrahedral distortion showing that only one minimal structure is favored for $[Ni(dppe)_2]^{2+}$, in line with ^{31}P NMR spectroscopic data (vide supra) and extended Hückel calculations on $[Ni(PH_3)_4]^{2+}$.[14]

Discussion

The electronic and conformational studies described in the preceding section have been performed to investigate the steric and electronic influence of *para*-$SiMe_2CH_2CH_2C_6F_{13}$-functionalization of the ligands on the metal center in a range of catalytically relevant group 10 metal complexes. The similar electron binding energies for fluorous and nonfluorous complexes found by XPS and the similar Ni, P, and Cl Mulliken populations calculated for $NiCl_2$(dppe) and **3c** by DFT show that any inductive electronic effect of the (1*H*,1*H*,2*H*,2*H*-perfluoroalkyl)dimethylsilyl-substituent exerted on the metal center is negligible. Differences in the onsets of the reduction potentials observed by cyclovoltammetry and in the shake-up satellite intensity in the XPS spectra were found for fluorous and nonfluorous nickel complexes. These observations, however, can be explained by steric rather than inductive electronic effects:

It is known that nickel complexes are configurationally more flexible than the corresponding palladium and platinum complexes due to lower crystal field stabilization energy. For example, X-ray crystallographic structures of both tetrahedral and square planar forms of $NiCl_2(PPh_3)_2$ have been reported.[29] It was also mentioned that, for diamagnetic d^8 nickel complexes containing four phosphorus ligands, a variety of structures can be expected as a result of compromises between steric and electronic influences.[14] This makes the nickel complexes more sensitive toward nonbonding interactions with bulky substituents when compared to the corresponding palladium and platinum complexes, which in turn have strong preferences for the square planar conformation.

Tetrahedral distortion, possibly occurring upon attachment of *para*-$SiMe_2CH_2CH_2C_6F_{13}$ substituents, would also be in

(28) Perera, J. S. H. Q.; Frost, D. C.; McDowell, C. A. *J. Chem. Phys.* **1980**, *72*, 5151.

(29) (a) Brammer, L.; Stevens, E. D. *Acta Crystallogr.* **1989**, *45*, 400. (b) Corain, B.; Longato, B.; Angeletti, R. *Inorg. Chim. Acta* **1985**, *104*, 15. (c) Bruins Slot, H. J.; Havere, W. K. L.; Noordik, J. H.; Beurskens, P. T.; Royo, P. *J. Crystallogr. Spectrosc. Res.* **1984**, *14*, 623. (d) Garton, G.; Henn, D. E.; Powell, H. M.; Venanzi, L. M. *J. Chem. Soc.* **1963**, 3625.

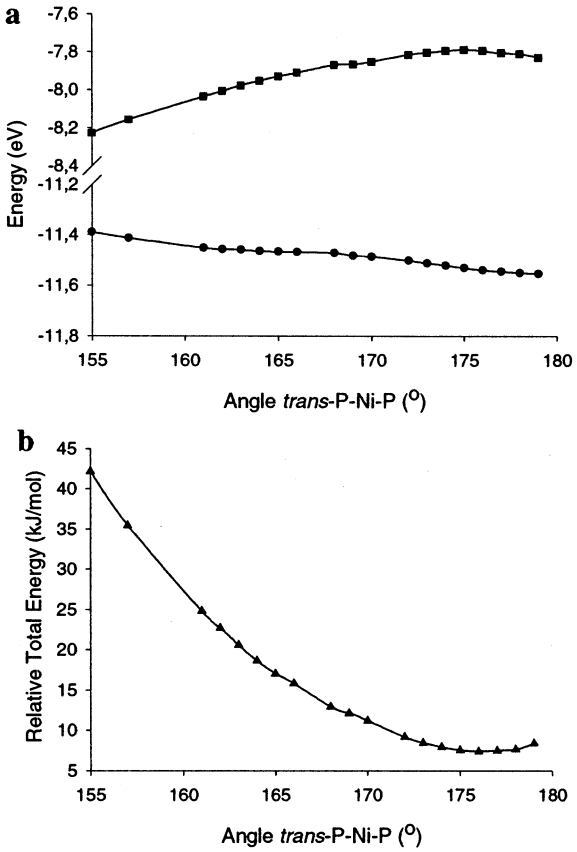

Figure 3. a. Energy levels of HOMO (●) and LUMO (■) of constrained, tetrahedrally distorted structures of $[Ni(dppe)_2]^{2+}$, calculated by DFT. b. Total energies of constrained, tetrahedrally distorted structures of $[Ni(dppe)_2]^{2+}$, relative to the nonconstrained minimum (−12.82283 MJ/mol), calculated by DFT.

agreement with the difference in the CV data obtained for $[Ni(dppe)_2](BF_4)_2$ and $[Ni(\mathbf{1c})_2](BF_4)_2$ (**7c**). Figure 3 shows that the energy of the LUMO of $[Ni(dppe)_2]^{2+}$ is lowered upon tetrahedral distortion. It was found that attachment of *p*-(1*H*,1*H*,2*H*,2*H*-perfluorooctyl)dimethylsilyl-groups to $[Ni(dppe)_2]^{2+}$ results in a reduction potential which is 0.25 V less negative compared to that of $[Ni(dppe)_2]^{2+}$. If it is assumed that this corresponds to an energy decrease of the LUMO of 0.25 eV and that the energies of the LUMO of **7c** follow a similar path upon tetrahedral distortion as calculated for $[Ni(dppe)_2]^{2+}$, then this would correspond by interpolation in Figure 3a to a tetrahedrally distorted structure with *trans*-P−Ni−P angles of 158°.

A tetrahedral distortion upon (1*H*,1*H*,2*H*,2*H*-perfluoroalkyl)dimethylsilyl-functionalization would also explain the higher shake-up satellite intensity observed in the XPS spectra of **3c** and **7c**, since the 3d−4s transition becomes more allowed in that case.[27] Consequently, mixtures consisting of square planar and tetrahedrally distorted geometries could be present in both the solid state (as in XPS measurements) and in solution (as in CV and ^{31}P NMR measurements). This would also be in agreement with the larger fwhm found in the XPS spectra of the fluorous nickel compounds.

In agreement with the single structure found for $[Ni(dppe)_2]^{2+}$ by ^{31}P NMR, no local minimum was found upon tetrahedral distortion of $[Ni(dppe)_2]^{2+}$ by DFT calculations. However, Figure 3 shows that the energy surface upon tetrahedral distortion of $[Ni(dppe)_2]^{2+}$ is relatively flat, allowing thermals distortions with *trans*-P−Ni−P angles up to 165° (4RT), demonstrating the geometrical flexibility of the nickel(II)-center. In contrast to $[Ni(dppe)_2]^{2+}$, **7c** contains 8 large, rigid perfluoroalkyl groups. Possibly, steric constraint might arise in **7c** due to the relatively small space available for the 8 rigid *p*-(1*H*,1*H*,2*H*,2*H*-perfluoroalkyl)dimethylsilyl-substituents. This might result in an energy surface for tetrahedral distortion which is different from the one calculated for $[Ni(dppe)_2]^{2+}$. Tetrahedral distortion, resulting in a more spherical distribution of the *para*-substituents, could relieve some of this steric constraint. When combined with the high flexibility of the nickel geometry, this could give rise to a second minimal, tetrahedrally distorted structure of **7c**.

It remains intriguing that only fluorous **7c** and **3c** and not nonfluorous **7b**, all three of them containing a large *p*-alkyldimethylsilyl-substituent, show differences in XPS and CV compared to their nonsubstituted analogues. This might be related to steric constraint arising from the larger size of a fluorine atom compared to a hydrogen atom and/or the lower flexibility of perfluoroalkyl tails compared to perprotioalkyl tails,[2] leading to distortion from planarity of the geometry around the nickel atom.

Although no significant differences between fluorous and nonfluorous palladium and platinum complexes were observed by XPS and ^{195}Pt NMR, slightly lower $^1J_{PtP}$ coupling constants were observed upon both trimethylsilyl- and (1*H*,1*H*,2*H*,2*H*-perfluoroalkyl)silyl-functionalization (vide supra). Inductive electronic effects as well as severe tetrahedral distortion are not likely to occur for platinum complexes, and no indications for these phenomena were found by XPS or ^{195}Pt NMR. It seems therefore that the somewhat lower $^1J_{PtP}$ coupling constants are most probably caused by subtle steric effects, e.g., causing a widening of the intervalence angles around the phosphorus atom (distortion to sp^2 hybridization), and/or by changes in the P−Pt−P bite angle. Therefore, the Hammett parameters for *para*-$SiMe_2CH_2CH_2CF_3$ and *para*-$SiMe_2CH_2CH_2C_6F_{13}$ (0.08 and 0.10, respectively), that can be determined from the $^1J_{PtP}$ coupling constants of *cis*-$[PtCl_2(\mathbf{2})]$ by interpolation in a linear plot of the Hammett constants and the $^1J_{PtP}$ coupling constant for several *cis*-$PtCl_2[P\text{-}(C_6H_4\text{-}4\text{-}R)_3]_2$ complexes,[20] seem to be unreliable and are not in agreement with the DFT calculations on **3** (Hammett parameter $\sigma_p = 0.00$ for both substituents).

Conclusions

Fluorous derivatives of dppe and PPh_3, containing the *para*-$SiMe_{3-b}(CH_2CH_2-)_b$-spacer, show similar complexation behavior toward Ni, Pd, and Pt compared to their nonsubstituted analogues. Using the fluorous diphosphines, both neutral and ionic group 10 metal complexes with preferential solubility in perfluorinated solvents were synthesized. NMR spectroscopy, XPS data, DFT calculations, and to a lesser extent cyclic voltammetry indicate that the *para*-(1*H*,1*H*,2*H*,2*H*-perfluoroalkyl)dimethylsilyl-function-

alization of the phosphine ligand does not influence the electronic properties of the metal center in these group 10 complexes. It can thus be concluded that, by using a silicon spacer, substantial fluorophilicity has been introduced in group 10 metal diphosphine complexes with minimal consequences for the electronic properties of the metal center. So far this has been difficult to achieve for diphosphines complexes. The metal complexes are potentially interesting for fluorous biphasic separation strategies.

Experimental Section

General. All experiments were performed in a dry dinitrogen atmosphere using standard Schlenk techniques. Solvents were stored over sodium benzophenone ketyl or CaH_2 and distilled before use. Fluorinated solvents (*c*-$C_6F_{11}CF_3$ (Lancaster), FC-72 and $CF_3C_6H_5$ (Acros)) were degassed and stored under dinitrogen atmosphere. Derivatives of dppe (**1a**−**f**),[10] **2b**,[12c] $[Ni(MeCN)_6](BF_4)_2 \cdot 1/2MeCN$,[30] $[Pd(MeCN)_4](BF_4)_2$,[31] $PdCl_2(COD)$,[32] and $PtCl_2(COD)$[33] were prepared according to previously reported procedures. Other chemicals were obtained from commercial suppliers (Acros, Aldrich, Lancaster) and used as delivered. Microanalyses were carried out by H. Kolbe, Mikroanalytisches Laboratorium, Mülheim an der Ruhr. ^{19}F NMR spectra were externally referenced against $CFCl_3$ ($\delta = 0$ ppm), ^{31}P NMR spectra against H_3PO_4 ($\delta = 0$ ppm), and ^{195}Pt NMR spectra against a 1 M solution of $NaPtCl_6$ in D_2O ($\delta = 0$ ppm).

The XPS data were obtained with a Vacuum Generators XPS system, using a CLAM-2 hemispherical analyzer for electron detection. Nonmonochromatic Al Kα X-ray radiation was used for exciting the photoelectron spectra using an anode current of 20 mA at 10 keV. The pass energy of the analyzer was set at 50 eV. The survey scan was taken with a pass energy of 100 eV.

Electrochemical measurements were performed in an electrochemical cell where a nitrogen atmosphere was maintained. The measurements were performed with a conventional three-electrode configuration using platinum electrodes and a Ag/AgCl reference electrode. Cyclovoltammetric measurements were carried out in $MeCN/CH_2Cl_2$ (1:1 v/v) containing the supporting electrolyte (0.05 M Bu_4NPF_6). The reference electrode was separated from the solution by a glass frit. Peaks were referenced to the Fc/Fc^+ couple in $MeCN/CH_2Cl_2$ (1:1 v/v). An EG&G potentiostat/galvanostat model 263A was used, connected to model 270/250 Research Electrochemistry Software (version 4.23).

All calculations were perfomed using Gamess-UK SGI version 6.3.[34] The DFT is invoked using the following keywords: DFT B3LYP. The keyword B3LYP selects the hybrid exchange-correlation energy functional due to Becke.[35] The quadrature grids are designed to obtain a relative error of less than 1.0×10^{-6} in the number of electrons per atom. These grids are constructed from the logarithmic radial grid[36] and Gauss−Legendre angular grid, using the SSF weighting scheme with screening[37] and MHL angular grid pruning.[36b] The gradient of the energy is evaluated without considering the gradient of the quadrature weights and grid points. The basis set was the double zeta basis double due to Schafer, Horn, and Ahlrichs;[38] Cartesian Gaussians were used throughout.

1,2-Bis[bis{4-((dimethyloctyl)silyl)phenyl}phosphino]-ethane (1b). A solution of 0.74 g of 1,2-bis[bis(4-bromophenyl)-phosphino]ethane (1.04 mmol) in THF (20 mL) was cooled to −90 °C, and 5.5 mL of a solution of *t*-BuLi (1.5 M; 8.3 mmol) was added. After the mixture was stirred for 30 min while the temperature was kept lower than −60 °C, 0.86 g (4.15 mmol) of $C_8H_{17}SiMe_2Cl$ was added. After the mixture was heated to room temperature, all volatiles were evaporated. The residue was dissolved in CH_2Cl_2/degassed water. The organic layer was separated, dried on $MgSO_4$, and evaporated to dryness, yielding 1.04 g (93%) of a clear light brown oil. Anal. Calcd for $C_{66}H_{112}P_2Si_4$: C 73.41, H 10.45. Found: C 69.67, H 10.93. ^1H NMR (200 MHz, $CDCl_3$): δ 0.28 (s, 24 H), 0.77 (m, 8 H), 0.92 (t, $^3J_{HH} = 3.4$ Hz, 12 H), 1.29 (m, 48 H), 2.16 (ps t, $J = 3.5$ Hz, 4H), 7.35−7.54 (m, 16 H). ^{31}P NMR ($CDCl_3$, 81.0 MHz): δ −12.0.

Tris[4-{dimethyl(3,3,3-trifluoropropyl)silyl}phenyl]phosphine (2a). To a solution of tris(4-bromophenyl)phosphine (0.56 g; 1.12 mmol) in Et_2O (20 mL) was added *t*-BuLi (6.7 mmol; 4.5 mL 1.5 M solution in pentane) at −78 °C. After stirring for 10 min, the reaction mixture was quenched with chlorodimethyl(3,3,3-trifluoropropyl)silane (0.64 g; 3.36 mmol). After the reaction mixture stirred for 3 h at room temperature, degassed water was added. After phase separation, drying of the organic layer on $MgSO_4$, filtration, and evaporation of the solvent, 0.70 g (86%) of a white solid was obtained. Anal. Calcd for $C_{33}H_{42}F_9PSi_3$: C 54.68, H 5.84, P 4.27. Found: C 54.82, H 5.74, P 4.36. ^1H NMR (200 MHz, $CDCl_3$): δ 0.31 (s, 18H), 0.95 (m, 6H), 1.95 (m, 6H), 7.30 (m, 6H), 7.46 (m, 6H). ^{19}F NMR (282 MHz, $CDCl_3$): δ −69.1 (t, $^3J_{HF} = 9.9$ Hz). ^{31}P NMR (81 MHz, $CDCl_3$): δ −4.9.

General Procedure for Synthesis of 3. A solution of the dppe derivative in an appropriate solvent was added to $NiCl_2 \cdot 6H_2O$ dissolved in EtOH or $EtOH/CF_3C_6H_5$ (**3f**). All volatiles were evaporated in vacuo, and the product was washed with EtOH (**3c**, **3d**, and **3e**) or purified in a FC-72/EtOH biphasic system (**3f**). Compound **3a** was not purified any further.

3a. Compound **1a** (0.30 g; 0.44 mmol) dissolved in $EtOH/CH_2Cl_2$ (50 mL; 4:1 v/v) and $NiCl_2 \cdot 6H_2O$ (0.10 g; 0.44 mmol) yielded 0.35 g of a red solid (94%). Anal. Calcd for $C_{38}H_{56}Cl_2NiP_2Si_4$: C 55.88, H 6.91, P 7.58. Found: C 55.72, H 6.83, P 7.63. ^1H NMR (200 MHz, $CDCl_3$): δ 0.30 (s, 36H), 2.10 (m, 4H), 7.61 (m, 8H), 7.91 (m, 8H). ^{31}P NMR (81 MHz, $CDCl_3$): δ 57.9.

3c. Compound **1c** (0.56 g; 0.28 mmol) dissolved in $EtOH/CH_2Cl_2$ (50 mL; 4:1 v/v) and $NiCl_2 \cdot 6H_2O$ (66 mg; 0.28 mmol) yielded 0.51 g of a red solid (85%). Anal. Calcd for $C_{66}H_{60}Cl_2F_{52}NiP_2Si_4$: C 36.96, H 2.82, P 2.89. Found: C 37.02, H 2.94, P 3.02. ^1H NMR (200 MHz, $CDCl_3$): δ 0.36 (s, 24H), 1.02 (m, 8H), 2.06 (m, 12H), 7.61 (m, 8H), 7.97 (m, 8H). ^{31}P NMR (81 MHz, $CDCl_3$): δ 58.1. ^{19}F NMR (282.4 MHz, $CDCl_3$): δ −126.6 (m, 8F), −123.5 (m, 8F), −123.3 (m, 8F), −122.4 (m, 8F), −116.3 (m, 8F), −81.3 (m, 12F).

3d. Compound **1d** (0.96 g; 0.40 mmol) dissolved in $CF_3C_6H_5$ and $NiCl_2 \cdot 6H_2O$ (95 mg; 0.40 mmol) yielded 0.91 g of a red solid

(30) Sen, A.; Ta−Wang, L. *J. Am. Chem. Soc.* **1981**, *103*, 4627.
(31) Ittel, S. D. In *Inorganic Synthesis*; MacDarmid, A. G., Ed.; Mcgraw-Hill: New York, 1977; Vol. 17, p 117.
(32) Frye, H.; Kuljian, E.; Viebrock, J. *Inorg. Chem.* **1965**, *4*, 1499.
(33) Drew, D.; Doyle, J. R. *Inorg. Synth.* **1990**, *28*, 346.
(34) Guest, M. F.; van Lenthe, J. H.; Kendrick, J.; Schöffel, K.; Sherwood, P.; Harrison, R. J. *GAMESS-UK version 6.3, a package of ab initio programs*; 2001. This was produced with contributions from Amos, R. D.; Buenker, R. J.; Dupuis, M.; Handy, N. C.; Hillier, I. H.; Knowles, P. J.; Bonacic-Koutecky, V.; von Niessen, W.; Saunders: V. R.; Stone, A. J. It is derived from the original *GAMESS* code: Dupuis, M.; Spangler, D.; Wendolowski, J. *GAMESS*; NRCC Software Catalog, 1980; Vol. 1, Program QG01.
(35) Becke, A. D. *J. Chem. Phys.* **1993**, *98*, 5648.
(36) (a) Mura, M. E.; Knowles, P. J. *J. Chem. Phys.* **1996**, *104*, 9848. (b) Murray, C. W.; Handy, N. C.; Laming, G. J. *Mol. Phys.* **1993**, *78*, 997.
(37) Stratmann, R. E.; Scuseria, G. E.; Frisch, M. J. *Chem. Phys. Lett.* **1996**, *257*, 213.
(38) Schafer, A.; Horn, H.; Ahlrichs, R. *J. Phys. Chem.* **1992**, *97*, 2571.

(89%) Anal. Calcd for $C_{74}H_{60}Cl_2F_{68}NiP_2Si_4$: C 34.92, H 2.38, F 50.76. Found: C 35.11, H 2.51, F 50.55. ^{1}H NMR (200 MHz, $CDCl_3$): δ 0.37 (s, 24H), 1.03 (m, 8H), 2.07 (m, 12H), 7.61 (m, 8H), 7.98 (m, 8H). ^{31}P NMR (81 MHz, $CDCl_3$): δ 58.1. ^{19}F NMR (282.4 MHz, $CDCl_3$): δ −126.6 (m, 8F), −123.5 (m, 8F), −123.2 (m, 8F), −122.4 (m, 24 F), −116.4 (m, 8F), −81.3 (m, 12 F).

3e. Compound **1e** (2.29 g; 0.69 mmol) dissolved in EtOH/$CF_3C_6H_5$ (100 mL; 1:1 v/v) and $NiCl_2\cdot 6H_2O$ (163 mg; 0.69 mmol) yielded 2.13 g of a red waxy solid (89%). Anal. Calcd for $C_{94}H_{64}Cl_2F_{104}NiP_2Si_4$: C 32.51, H 1.86, P 1.78. Found: C 32.38, H 1.94, P 1.88. ^{1}H NMR (200 MHz, $CDCl_3$): δ 0.34 (br, 12H), 1.06 (br, 16 H), 2.02 (br, 20 H), 7.4−8.2 (br, 16H). ^{31}P NMR (81 MHz, $CDCl_3$): δ 58.0.

3f. Compound **1f** (1.68 g; 0.36 mmol) dissolved in $CF_3C_6H_5$ and $NiCl_2\cdot 6H_2O$ (85 mg; 0.36 mmol) yielded 1.50 g of a red oil (87%). Anal. Calcd for $C_{122}H_{68}Cl_2F_{156}NiP_2Si_4$: C 30.52, H 1.43, P 1.29. Found: C 30.32, H 1.36, P 1.42. ^{1}H NMR (200 MHz, C_6D_6/FC-72 1:1 v/v): δ 1.01 (br, 24H), 1.96 (br, 28H), 7.2−8.2 (br, 16H). ^{31}P NMR (81 MHz, $CDCl_3/CF_3C_6H_5$ 1:1 (v/v)): δ 57.8.

General Procedure for Synthesis of 4. A solution of **1** in CH_2Cl_2 (**1a**, **1c**) or PFMCH (**1f**) was added to a solution of $PdCl_2$(COD) in CH_2Cl_2. After the reaction mixture stirred overnight, all solvent was evaporated in vacuo.

4a. Compound **1a** (0.16 g; 0.22 mmol) and $PdCl_2$(COD) (64 mg; 0.22 mmol) yielded 0.16 g (81%) of a yellow solid. Anal. Calcd for $C_{38}H_{56}Cl_2P_2PdSi_4$: C 52.80, H 6.53, P 7.17. Found: C 52.55, H 6.46, P 7.25. ^{1}H NMR (200 MHz, $CDCl_3$): δ 0.27 (s, 24H), 2.44 (m, 4H), 7.59 (m, 8H), 7.82 (m, 8H). ^{31}P NMR (81 MHz, $CDCl_3$): δ 64.7.

4c. Compound **1c** (0.27 g; 0.13 mmol) and $PdCl_2$(COD) (38 mg; 0.13 mmol) yielded 0.27 g (95%) of a yellow solid. Anal. Calcd for $C_{66}H_{60}Cl_2F_{52}P_2PdSi_4$: C 36.15, H 2.76, P 2.83. Found: C 36.26, H 2.70, P 2.99. ^{1}H NMR (200 MHz, $CDCl_3$): δ 0.35 (s, 24H), 1.01 (m, 8H), 2.02 (m, 8H), 2.50 (m, 4H), 7.61 (m, 8H), 7.90 (m, 8H). ^{31}P NMR (81 MHz, $CDCl_3$): δ 64.5. ^{19}F NMR (282.4 MHz, $CDCl_3$): δ −126.7 (m, 8F), −123.6 (m, 8F), −123.4 (m, 8F), −122.5 (m, 8F), −116.4 (m, 8F), −81.4 (m, 12F).

4f. Compound **1f** (0.21 g; 44 μmol) and $PdCl_2$(COD) (13 mg; 44 μmol) yielded 0.21 g (90%) of a yellow oil. Anal. Calcd for $C_{122}H_{68}Cl_2F_{156}P_2PdSi_4$: C 30.22, H 1.41, P 1.28. Found: C 30.25, H 1.49, P 1.41. ^{1}H NMR (200 MHz, C_6D_6/PFMCH 1:1 (v/v)): δ 0.86 (br, 24H), 1.85 (br, 28H), 6.8−8.0 (br, 16H). ^{31}P NMR (81 MHz, C_6D_6/PFMCH 1:1 (v/v)): δ 62.2.

General Procedure for Synthesis of 5. A solution of 1 equiv of **1** or 2 equiv of monophosphine in CH_2Cl_2 was added to a solution of 1 equiv of $PtCl_2$(COD) in CH_2Cl_2. After the reaction mixture stirred overnight, all solvent was evaporated in vacuo.

5a. Compound **1a** (0.15 g; 0.22 mmol) and $PtCl_2$(COD) (81 mg; 0.22 mmol) yielded 0.19 g (92%) of a white solid. Anal. Calcd for $C_{38}H_{56}Cl_2P_2PtSi_4$: C 47.88, H 5.92, P 6.50. Found: C 47.90, H 6.05, P 6.39. ^{1}H NMR (200 MHz, $CDCl_3$): δ 0.30 (s, 36H), 2.37 (m, 4H), 7.60 (m, 8H), 7.81 (m, 8H).

5c. Compound **1c** (0.45 g; 0.22 mmol) and $PtCl_2$(COD) (84 mg; 0.22 mmol) yielded 0.46 g (93%) of a white solid. Anal. Calcd for $C_{66}H_{60}Cl_2F_{52}P_2PtSi_4$: C 34.75, H 2.65, P 2.72. Found: C 34.61, H 2.70, P 2.80. ^{1}H NMR (200 MHz, $CDCl_3$): δ 0.34 (s, 24H), 1.00 (m, 8H), 2.02 (m, 8H), 2.36 (m, 4H), 7.56 (m, 8H), 7.85 (m, 8H). ^{19}F NMR (282.4 MHz, $CDCl_3$): δ −126.7 (m, 8F), −123.6 (m, 8F), −123.4 (m, 8F), −122.5 (m, 8F), −116.4 (m, 8F), −81.4 (m, 12F).

5e. Compound **1e** (0.41 g; 0.12 mmol) and $PtCl_2$(COD) (46 mg; 0.12 mmol) yielded 0.39 g (91%) of a waxy white-yellow solid. Anal. Calcd for $C_{94}H_{64}Cl_2F_{104}P_2PtSi_4$: C 31.28, H 1.79, F 54.74. Found C 31.04, H 1.89, F 54.29. ^{1}H NMR (200 MHz, C_6D_6/FC-72 1:1 v/v): δ 0.00 (s, 12H), 0.83 (br, 16H), 1.84 (br, 16H), 7.15 (br, 8H), 7.96 (br, 8H).

***cis*-$PtCl_2[P(4\text{-}C_6H_4\text{-}SiMe_2CH_2CH_2CF_3)_3]_2$ (6a).** Compound **2a** (0.25 g; 0.35 mmol) and $PtCl_2$(COD) (64.6 mg; 0.17 mmol) yielded 0.24 g (82%) of a white solid. Anal. Calcd for $C_{66}H_{84}Cl_2F_{18}P_2PtSi_6$: C 46.20, H 4.93, P 3.61. Found: C 46.16, H 4.98, P 3.68. ^{1}H NMR (200 MHz, $CDCl_3$): δ 0.33 (s, 36H), 0.96 (m, 12H), 1.96 (m, 12H), 7.28 (m, 12H), 7.45 (m, 12H).

***cis*-$PtCl_2[P(4\text{-}C_6H_4\text{-}SiMe_2CH_2CH_2C_6F_{13})_3]_2$ (6b).** Compound **2b** (0.53 g; 0.36 mmol) and $PtCl_2$(COD) (67.0 mg; 0.18 mmol) yielded 0.53 g (91%) of a white solid. Anal. Calcd for $C_{96}H_{84}Cl_2F_{78}P_2PtSi_6$: C 35.85, H 2.63, P 1.93. Found: C 35.70, H 2.71, P 1.85. ^{1}H NMR (200 MHz, $CDCl_3$): δ 0.29 (s, 36H), 0.94 (m, 12H), 1.92 (m, 12H), 7.46 (m, 24H).

General Procedure for Synthesis of 7. A solution of **1** in CH_2Cl_2 was added to a solution of $[Ni(MeCN)_6](BF_4)_2\cdot 1/2MeCN$ in MeCN. After the reaction mixture stirred for 2 h, all volatiles were evaporated in vacuo. The residue was dissolved in CH_2Cl_2, filtered, and evaporated to dryness.

7a. Compound **1a** (0.10 g; 0.14 mmol) and $[Ni(MeCN)_6](BF_4)_2\cdot 1/2MeCN$ (35 mg; 70 μmol) yielded 0.10 g (89%) of a yellow solid. Anal. Calcd for $C_{76}H_{112}B_2F_8NiP_4Si_8$: C 56.82, H 7.03, P 7.71. Found: C 56.70, H 6.92, P 7.56. ^{1}H NMR (200 MHz, CD_3CN): δ 0.36 (s, 72H), 2.71 (m, 8H), 7.06 (m, 16H), 7.51 (m, 16H). ^{31}P NMR (81 MHz, CD_3CN): δ 54.5.

7b. Compound **1b** (0.28 g; 0.26 mmol) and $[Ni(MeCN)_6](BF_4)_2\cdot 1/2MeCN$ (65 mg; 0.13 mmol) yielded 0.27 g (87%) of an orange oil. Anal. Calcd for $C_{132}H_{224}B_2F_8NiP_4Si_8$: C 66.28, H 9.44, P 5.18. Found: C 66.20, H 9.35, P 5.29. ^{1}H NMR (200 MHz, $CDCl_3$): δ 0.24 (s, 48H), 0.73 (m, 16H), 0.87 (br, 16H), 1.25 (br, 96H), 2.92 (m, 8H), 7.1−7.5 (m, 32H). ^{31}P NMR (81 MHz, $CDCl_3$): δ 54.9.

7c. Compound **1c** (0.68 g; 0.34 mmol) and $[Ni(MeCN)_6](BF_4)_2\cdot 1/2MeCN$ (85 mg; 0.17 mmol) yielded 0.67 g (93%) of a yellow solid, which was recrystallized from MeCN and hexane. Anal. Calcd for $C_{132}H_{120}B_2F_{112}NiP_4Si_8$: C 37.19, H 2.84, P 2.91. Found: C 37.09, H 2.85, P 3.04. ^{1}H NMR (200 MHz, CD_3CN): δ 0.36 (s, 48H), 1.05 (m, 16H), 2.08 (m, 16H), 2.71 (m, 8H), 6.9−7.6 (m, 32H). ^{31}P NMR (81 MHz, CD_3CN): δ 54.5 (s, 3P). ^{19}F NMR (282 MHz, CD_3CN): δ −150.7 (m, 8F), −125.7 (m, 16F), −122,4 (m, 32F), −121.4 (m, 16F), −115.1 (m, 16F), −80.6 (m, 24F).

General Procedure for Synthesis of 8. A solution of **1** in CH_2Cl_2 was added to a solution of $[Pd(MeCN)_4](BF_4)_2$ in MeCN. After the reaction mixture for 2 h, all volatiles were evaporated in vacuo. The residue was dissolved in CH_2Cl_2, filtered, and evaporated to dryness.

8a. Compound **1a** (217 mg; 0.30 mmol) and $[Pd(MeCN)_4](BF_4)_2$ (67 mg; 0.15 mmol) yielded 240 mg (97%) of a light yellow solid. Anal. Calcd for $C_{76}H_{112}B_2F_8P_4PdSi_8$: C 55.18, H 6.82, P 7.49. Found: C 54.94, H 6,73, P 7.58. ^{1}H NMR (200 MHz, CD_3CN): δ 0.20 (s, 72 H), 3.02 (m, 8H), 7.20 (m, 16H), 7.41 (m, 16H). ^{31}P NMR (81 MHz, $CDCl_3$): δ 56.5.

8c. Compound **1c** (294 mg; 0.146 mmol) and $[Pd(MeCN)_4](BF_4)_2$ (32.4 mg; 73 μmol) yielded 292 mg (93%) of a light yellow solid. Anal. Calcd for $C_{132}H_{120}B_2F_{112}P_4PdSi_8$: C 36.78, H 2.81, P 2.87. Found: C 36.91, H 2.90, P 2.97. ^{1}H NMR (200 MHz, $CDCl_3$): δ 0.29 (s, 48H), 1.07 (m, 16H), 2.10 (m, 16H), 2.92 (m, 8H), 6.9−7.6 (m, 32H). ^{31}P NMR (81 MHz, $CDCl_3$): δ 56.8. ^{19}F NMR (282 MHz, CD_3CN): δ −155.2 (m, 8F), −130.1 (m, 16F), −126.8 (m, 32F), −125.9 (m, 16F), −199.5 (m, 16F), −85.1 (m, 24F).

Solubility Studies of $NiCl_2$(dppe) and 3. Saturated solutions were prepared by stirring the nickel complex in the appropriate solvent for 30 min at 25 °C. A sample was taken after the mixture

was allowed to settle and the mass of the sample was determined. All solvent was removed in vacuo, and the residue was kept under vacuum (0.1 mbar) for 15 h upon which the weight was constant within ±1 mg and the weight of the residue was determined.

Determination of Partition Coefficients. A known amount of **3** (between 9 and 33 μmol) was dissolved in a biphasic system containing PFMCH (2.000 ± 0.002 mL) and toluene (2.000 ± 0.002 mL). The mixture was stirred until all of the compound had dissolved and then equilibrated at 0 °C. When two clear layers were obtained, an aliquot (500 ± 2 μL) was removed from each layer by syringe. This was evaporated to dryness, and the residue was kept under vacuum (0.1 mbar) for 15 h upon which the weight was constant within ±1 mg. Subsequently, the weight of the residue was determined.

Acknowledgment. ATOFINA Vlissingen B.V. and the Dutch Ministry for Economic Affairs (SENTER/BTS) are gratefully acknowledged for their financial support. The Stichting Nationale Computerfaciliteiten (National Computing Facilities Foundation, NCF) and NWO are acknowledged for the use of supercomputer facilities. Also, the staff of SARA is thanked for their help with the DFT calculations.

Supporting Information Available: Gamess output file listing energy values, *z*-matrix, orbital energies, and Mulliken populations for geometry-optimized $[Ni(dppe)_2]^{2+}$. This material is available free of charge via the Internet at http://pubs.acs.org.

IC025770L